Position-defect-induced reflection, trapping, transmission, and resonance in quantum walks

Z. J. Li,[1,2,*] J. A. Izaac,[2] and J. B. Wang[2,†]

[1]*Institute of Theoretical Physics, Shanxi University, Taiyuan, 030006, China*

[2]*School of Physics, The University of Western Australia, Crawley, WA 6009, Australia*

(Received 1 November 2012; published 17 January 2013)

We investigate the scattering properties of quantum walks by considering single and double position defects on a one-dimensional line. This corresponds to introducing, at designated positions, delta potential defects for continuous-time quantum walks and phase-defect Hadamard coins for discrete time quantum walks. The delta potential defects can be readily considered as potential barriers in discrete position space, which affect the time evolution of the system in a similar way as the quantum wave-packet dynamics in a continuous position space governed by Schrödinger's equation. Although there is no direct analogy of potential barriers in the theoretical formulation of discrete time quantum walks, in this paper we show that the phase defects in the coin space can be utilized to provide similar scattering effects. This study provides means of controlling the scattering properties of quantum walks by introducing designated position-dependent defects.

DOI: 10.1103/PhysRevA.87.012314 PACS number(s): 03.67.Lx, 05.40.Fb, 05.45.Mt

I. INTRODUCTION

Quantum walks are the quantum analog to the classical random walk, extended to take into account superposition, interference, and quantum correlations. It provides a comprehensive framework to study quantum dynamics in discrete and structured space. Compared to the classical random walk, quantum walks exhibit markedly different behavior; for instance, a quantum walk can propagate quadratically faster than its classical counterpart, is a time-reversible process rather than a memoryless Markov process, and results in a probability distribution drastically different from the classically expected Gaussian [1]. As with classical random walks, there are two related but fundamentally different formulations of quantum walks—the discrete-time quantum walk (DTQW) [2] and the continuous-time quantum walk (CTQW) [3]. Due to their unintuitive dynamical behavior, quantum walks have been extensively explored over the past decade, which may provide methods of modeling complex biological systems [4,5] or hold the key to radical new quantum algorithms [1,6–11].

Disorder is unavoidable in most quantum systems. The evolution of quantum walks in a discrete environment with static and dynamic disorders have been studied both theoretically and experimentally, demonstrating a variety of interesting dynamics such as ballistic and diffusive spreading [12–16], as well as Anderson and bound-state localization [15–23]. In CTQW, disorder can be represented by position- or time-dependent potential defects in the diagonal elements of the transition matrix. The position dependence can be chosen as a random distribution within a certain range [19] or as a function distribution such as a Cauchy distribution [15], while time dependence can also be either random or regular [15]. In DTQW, disorder is introduced through the coin operator; the position-dependent coin provides static disorder, while the time-dependent coin gives rise to dynamic disorder [13,23]. In this paper, we study the scattering properties of quantum walks, including reflection, trapping, and resonance transmission for both CTQW and DTQW with a wide range of defect settings. In particular, we investigate the roles played by the potential defects in CTQW and the phase defects in DTQW with respect to the control of quantum walk behaviors. Furthermore, we extend the work of previous studies (which were primarily concerned with quantum walkers initially localized at a defect) to consider an initially free quantum walk interacting with multiple defects.

In what follows we present, in Sec. II, an introductory overview of CTQW and DTQW, and describe the single and double point-defect model. In Sec. III, we give the evolution properties of QW's for three initial cases: (1) the particle lies at the node containing the defect (the "distinguished node"), (2) the particle lies to the side of the defect, and (3) the particle lies between two defects. In Sec. III D, we investigate resonance transmission when two defects are present with specific separation. Finally, Sec. IV contains our conclusions.

II. QUANTUM WALK POINT-DEFECT MODEL

A. Continuous-time quantum walk

The continuous-time quantum walk was first posited by Farhi and Gutmann [3], motivated by a desire to establish a general framework to study coherent transport in discrete systems. The continuous-time quantum walk can be regarded as a quantization of the corresponding classical continuous-time random walk, with the system now evolving as per the Schrödinger equation rather than the Markovian master equation. As a result, classical probabilities are replaced by quantum probability amplitudes.

To illustrate, consider a continuous-time random walk on the discrete graph $G(V,E)$, composed of unordered vertices $j \in V$ and edges $e_i = (j,k) \in E$ connecting two vertices j and k. The transition rate matrix H is defined as

$$H_{jk} = \begin{cases} -\gamma_{jk} & \text{for } j \neq k \text{ if node } j \text{ is connected to node } k, \\ 0 & \text{for } j \neq k \text{ if node } j \text{ is not connected to node } k, \\ S_j & \text{for } j = k, \end{cases} \quad (1)$$

*zjli@sxu.edu.cn

†jingbo.wang@uwa.edu.au

where γ_{jk} is the probability per unit time for making a transition from node j to node k and for H to be conservative:

$$S_j = \sum_{k=1,k\neq j}^{N} \gamma_{jk}. \tag{2}$$

Classically, the state of the random walker is fully described by the probability distribution vector $\mathbf{P}(t)$, with its time evolution governed by the master equation

$$\frac{d\mathbf{P}(t)}{dt} = H\mathbf{P}(t),$$

which has the formal solution $\mathbf{P}(t) = \exp(-Ht)\mathbf{P}(0)$.

Extending the above description to the quantum realm involves replacing the real valued probability distribution vector $\mathbf{P}(t)$ with a complex valued wave function $|\psi(t)\rangle$, and adding the complex notation i to the evolution exponent; i.e.,

$$|\psi(t)\rangle = \exp(-iHt)|\psi(0)\rangle. \tag{3}$$

The quantum transition matrix H, often referred to as the system Hamiltonian, is required to be Hermitian and thus the above time evolution is unitary—guaranteeing that the norm of $|\psi(t)\rangle$ is conserved under CTQWs. The complex-valued state vector $|\psi(t)\rangle = \sum_j a_j(t)|j\rangle$, where $a_j(t) = \langle j|\psi(t)\rangle \in \mathbb{C}$, represents the probability amplitude of the walker being found at node $|j\rangle$ at time t, with $|a_j(t)|^2 = |\langle j|\psi(t)\rangle|^2$ the resulting probability.

For CTQWs on an infinite line, if each node is assumed to be connected only to its neighboring nodes by a constant transition rate $\gamma = 1$, the action of the corresponding Hamiltonian H_0 on the state vector $|\psi(t)\rangle$ leads to the inner product relationship

$$\langle j|H_0|\psi\rangle = 2\langle j|\psi\rangle - \langle j+1|\psi\rangle - \langle j-1|\psi\rangle. \tag{4}$$

Note that this equation is identical to the first-order finite difference approximation of the continuous-space operator $-\nabla^2$, which generates the time evolution of a free particle. In an analogous fashion we can regard the discrete position-space Hamiltonian H_0 given in Eq. (4) as the generator of a *free* CTQW. The significant difference in propagation behavior between these two systems arises due to the use of a discrete position space for the CTQW. It was shown by Manouchehri and Wang [24] that the discreteness of position space in Eq. (4) is a *necessary* condition for a CTQW to display its characteristic propagation behavior, as opposed to continuous-space wave-packet dispersion.

Symmetries that are present in continuous-space quantum systems, for instance invariance under spatial translation for free particles, can also be formulated for discrete space systems such as the continuous-time quantum walk on an infinite line. For instance, consider the discrete translational operator $\hat{T}_n$, which acts on the set of orthonormal vertex states $|j\rangle$ such that $\hat{T}_n|j\rangle = |j+n\rangle$. This operator is unitary, and as such can be written in the form $\hat{T}_n = e^{i\hat{k}n}$, where $\hat{k}$ is an Hermitian operator and the generator of the translation. In cases where the state of a quantum walker is invariant under spatial translation, the Hermiticity of $\hat{k}$ indicates that its eigenstates $|k\rangle = \sum_j e^{ikj}|j\rangle$ form a complete orthonormal basis, satisfying the eigenvalue equation $H_0|k\rangle = 2(1-\cos k)|k\rangle$ for $-\pi \leqslant k < \pi$. These eigenstates are useful when investigating resonance scattering in defect containing CTQW systems, as they provide a method of producing biased walks (since the initial state $|k\rangle$ has a well-defined "momentum" of k) similar to the continuous-space propagation of a plane wave. This allows its interaction multiple barriers to be considered in an analogous fashion.

Continuous-time quantum walks in the presence of absorbing barriers have previously been studied by Mülken *et al.* [25] and Agliari *et al.* [26]. Alternatively, walks in the presence of reflecting barriers (or defects) have been considered by Keating *et al.* [19] (using a Cauchy distributed defect) and Childs *et al.* [27] (a single defect), in the context of decoherence and algorithmic speedup, respectively. In this paper, we will be primarily concerned with implementing reflecting barriers, and characterizing the resulting behavior of quantum walking systems.

Keeping with the case of the CTQW on an infinite line, let us assume that there are defects present at particular nodes $|m\rangle$. This breaks the translational symmetry, and as such the walker can no longer be considered free. To account for these defects, the Hamiltonian matrix is modified in the following way:

$$H = H_0 + \Gamma, \quad \Gamma = \sum_m \Gamma_m |m\rangle\langle m|, \tag{5}$$

where we have introduced a real diagonal matrix Γ, with positive elements corresponding to defects or reflecting barriers placed at vertex $|m\rangle$ with strength Γ_m. The probability of the walker being found at node $|j\rangle$ at time t can thus be given by $|\langle j|e^{-iHt}|\psi(0)\rangle|^2$. In subsequent sections, we will consider reflecting barriers placed at specific nodes in order to investigate the scattering properties of quantum walks.

B. Discrete-time quantum walk

The discrete-time quantum walk also has a very similar mathematical formalism to that of its classical counterpart, and is implemented by a concatenation of coin operations and successive position shifts. It takes place in the Hilbert space $\mathcal{H}_\mathcal{P} \otimes \mathcal{H}_\mathcal{C}$ where, in the case of an infinite line, the position Hilbert space $\mathcal{H}_P$ is spanned by the position basis states $|i \in \mathbb{Z}\rangle$ and the "coin" Hilbert space $\mathcal{H}_C$ is spanned by the coin basis states $|c = 0,1\rangle$. A single step time evolution operator is given by

$$U = \left(\sum_c (|c\rangle\langle c| \otimes S_c)\right)\left(C \otimes \sum_i |i\rangle\langle i|\right), \tag{6}$$

where C is the coin operator, and S_c is a conditional translation operator defined as $S_c = \sum_i |i + (-1)^{c+1}\rangle\langle i|$. As with the continuous-time case, the system is described via the state vector $|\psi(t)\rangle = \sum_i \sum_c f_{ic}(t)|i\rangle \otimes |c\rangle$, with its evolution from initial state $|\psi(0)\rangle$ for discrete time t calculated via repeated use of the unitary operator given by Eq. (6), i.e.,

$$|\psi(t)\rangle = U^t|\psi(0)\rangle.$$

The major point of difference between the classical and quantum implementation of the discrete time walk is the use of a quantum, rather than classical, coin operator—with the result that the walker now has the possibility of being in a superposition of possible coin states $|c\rangle$ at every step. It should be noted that the resulting coherence is a source of most of the counterintuitive behavior of the DTQW; if the coin operator is applied randomly, or if we were to measure the coin state after

each time step, the superposition is destroyed and we recover the classical random walk.

When working with DTQWs, the coin degrees of freedom offer a wide range of control over the evolution of the walk. Of particular interest are position-dependent coin operators, as they act to break down the translational symmetry of the unitary operation in Eq. (6)—thus modification of the DTQW coin operation on a small number of nodes may be used to create an analogous system to the node-defect Hamiltonian in CTQW. It has been shown that the full range of possible DTQW evolutions obtained by different coin operators can also be obtained by fixing the coin operator, and choosing a range of different initial coin states [28]. Without loss of generality, one often restricts the coin operator to one with real coefficients; in the case of an unbiased quantum walk on a line, this leaves the Hadamard coin

$$C_H = \frac{1}{\sqrt{2}}\begin{bmatrix} 1 & 1 \\ 1 & -1 \end{bmatrix}$$

as the only possible choice. Taking this into account, the unitary operation in Eq. (6) is modified as follows:

$$U = \left(\sum_c (|c\rangle\langle c| \otimes S_c)\right)\left(\sum_j C_j (\otimes |j\rangle\langle j|\right), \qquad (7)$$

where the phase-defect Hadamard coin $C_j = e^{i\phi_j} C_H$ is applied at designated "defect nodes,"and $C_j = C_H$ otherwise.

III. LOCALIZATION, TRAPPING, AND REFLECTION

Localization and trapping by a single phase defect in discrete-time quantum walks have been studied in the literature, especially with the quantum walker starting at the defect position [13,23,29]. In this section we analyze the influence of single and double defects on the dynamical evolution of both discrete- and continuous-time quantum walks, with the quantum walker initially located at the origin but the defects at various positions. In particular, we investigate the physical interpretation of these defects in both CTQW and DTQW.

A. Single defect—localization

Let us first consider the case where a defect is present at the origin $|j = 0\rangle$ of an infinite line. Figure 1 shows that both CTQW and DTQW have similar probability distributions, with sharp peaks present at the origin. For comparison, the dashed line depicts the probability distribution of the free quantum walk without the defect. Further investigation shows that the amplitude of the peak, or alternatively the slope of standard deviation with time, is dependent on the strength of the defect potential for the CTQW [Fig. 2(a)]; the stronger the defect potential, the larger the probability amplitude at the origin. The peak in the probability distribution can be understood as bound-state localization, occurring due to the presence of the defect which generically generates a bound state in its surrounding [22,23]. The peak in the probability distribution is the fingerprint of this bound state [30]. Besides this large peak at the origin, two smaller peaks are also observed at the same locations as the ballistic peaks of the free quantum walk—inferring that the linear relationship between the states' standard deviation with time, $\sigma \sim t$, remains unchanged in spite of a drastically reduced amplitude for the two smaller peaks.

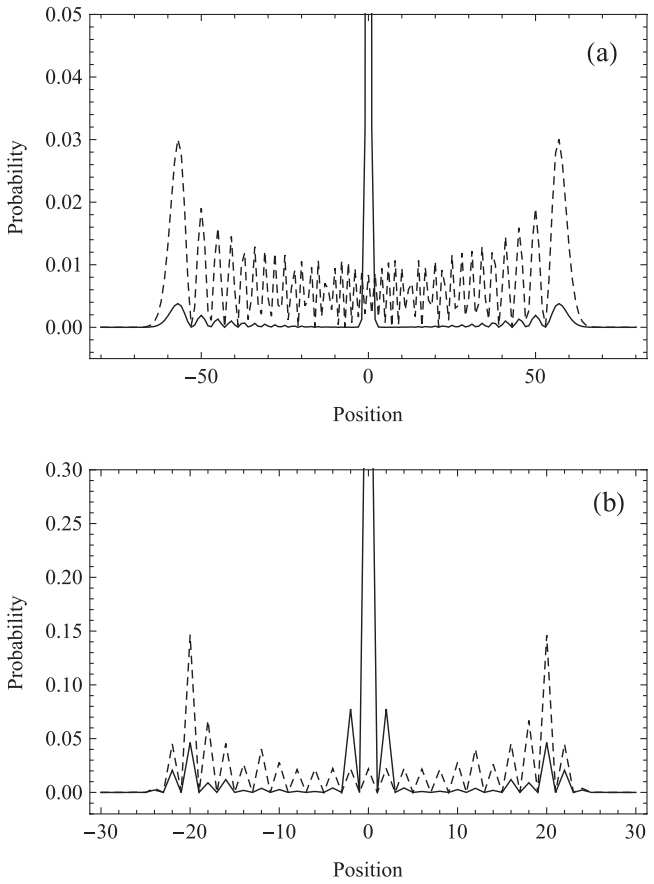

FIG. 1. Probability distribution at time $t = 30$ for (a) CTQW with a defect potential $\Gamma_0 = 5$; (b) DTQW with a phase defect $\phi_0 = \pi$ and initial state $(|1\rangle + i|0\rangle)/\sqrt{2}$. The dashed line corresponds to a quantum walk without a defect.

The similarity of the DTQW and CTQW probability distributions in Fig. 1 suggests the possibility of manipulating the DTQW coin degrees of freedom, in an attempt to reproduce the CTQW physical effects attributed to the point defects. As discussed in Sec. II B, a wide range of possible evolutions of the DTQW can be produced by either varying the initial state (and using a fixed coin operator), or by varying the coin operator. Figure 2(b) displays the probability at the origin of the DTQW as a function of ϕ in the phase-defect Hadamard coin, for the initial coin states $(|1\rangle + i|0\rangle)/\sqrt{2}$, $|1\rangle$, and $|0\rangle$. It can be seen that the amplitude of the sharp peak depends strongly on the initial coin state of the system as well as the phase defect ϕ. For instance, using the initial coin state $(|1\rangle + i|0\rangle)/\sqrt{2}$, no localization is observed for any phase in the domain $\phi \in (0,\pi/4)$, since its overlap with the stationary bound state is close to zero. The probability at the origin is symmetric about $\phi_0 = 0$ for initial coin state $|0\rangle$ and $|1\rangle$, but not for initial state $(|1\rangle + i|0\rangle)/\sqrt{2}$. Also note that, for a given initial state, the phase defect ϕ appears to have the same function as the defect potential Γ in CTQW; both act to change the amplitude of the localization peak centered at the origin.

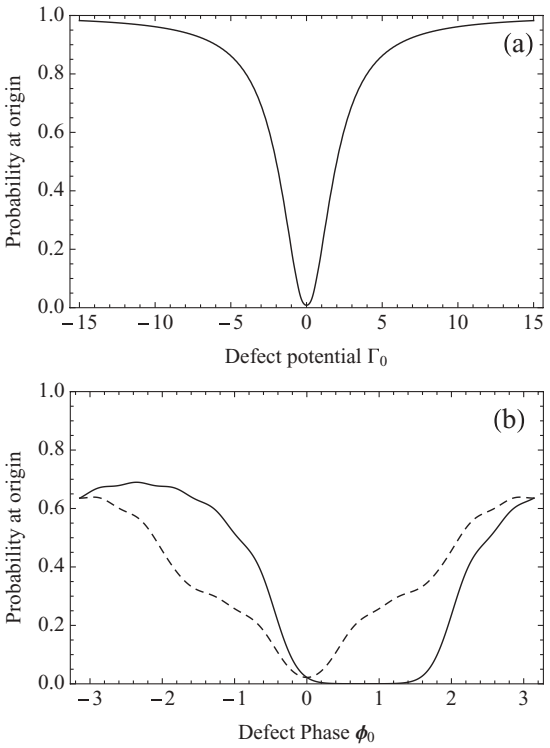

FIG. 2. Probability at the origin at time $t = 30$ as a function of (a) the defect potential Γ_0 for CTQW and (b) phase defect ϕ_0 for DTQW. In (b), the solid line corresponds to the initial coin state $(|1\rangle + i|0\rangle)/\sqrt{2}$, while the dashed line corresponds to the coin initial state $|1\rangle$ or $|0\rangle$.

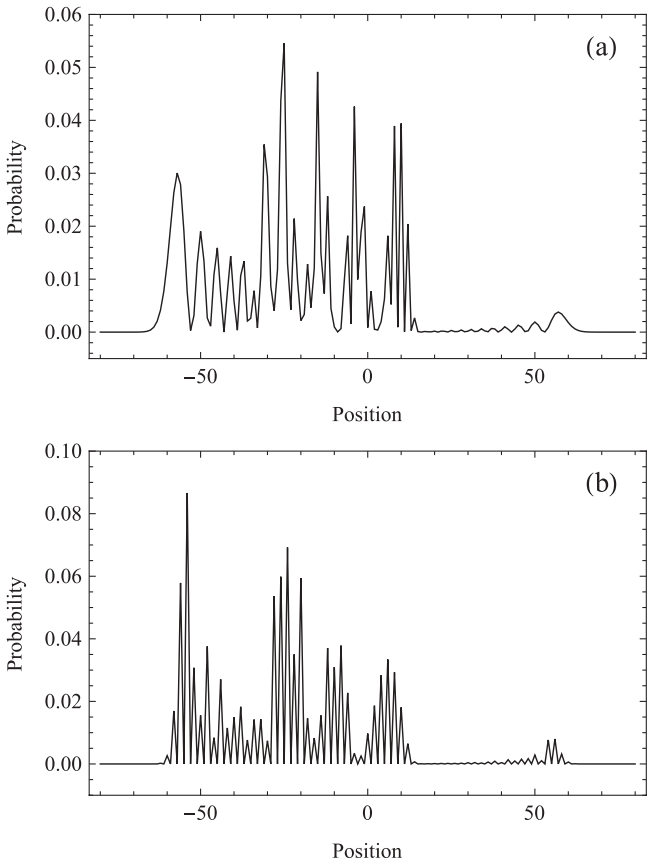

FIG. 3. Probability distribution for (a) CTQW at time $t = 30$ with a defect potential $\Gamma_{15} = 5$, and (b) DTQW after $t = 80$ steps with a phase defect $\phi_{15} = \pi$ and initial coin state $(|1\rangle + i|0\rangle)/\sqrt{2}$.

B. Single defect—reflection

Next, we discuss the case where the single point defect is located away from where the quantum walk starts. As an example, consider the quantum walk initially located at the origin with one defect $\Gamma_{15} = 5$ on an infinite line. The resulting probability distribution over the discrete position space at time $t = 30$ is shown in Fig. 3(a). Some important features to note: (1) it evolves symmetrically in both the left and right direction, which is identical to a "free"quantum walk prior to its interaction with the barrier; (2) upon interacting with the barrier, it is largely reflected with a small probability of transmission; (3) the transmitted component continues to evolve ballistically as per the free quantum walk; (4) the larger the defect potential, the weaker the transmitted amplitude, as shown in Fig. 4(a); and (5) the reflected component interferes with the original propagating component, resulting in a complex interference pattern and asymmetric distribution compared to the free quantum walker.

Figure 3(b) shows very similar propagation behavior in the case of DTQW, now using a phase-defect Hadamard coin $\phi_{15} = \pi$ and starting with initial state $(|1\rangle + i|0\rangle)/\sqrt{2}$. In this case, the transmission amplitude through the reflecting barrier can be manipulated by altering the phase value ϕ_{15} as shown in Fig. 4(b). It can be seen that the transmission amplitude is symmetric about $\phi_{15} = 0$ for initial coin state $|0\rangle$ or $|1\rangle$, but not for initial state $(|1\rangle + i|0\rangle)/\sqrt{2}$.

The above observations are very similar to the wave-packet dynamics in continuous position space when potential barriers are applied. In CTQW, the delta potential defects can be readily considered as potential barriers in discrete space, which bring about similar behaviors. Although there is no direct analogy of potential barriers in the theoretical formulation of DTQW, here we show that the additional coin degree of freedom can be utilized to provide similar scattering effects.

C. Double defects—trapping

Another scenario we can consider is to start the quantum walker at the origin between two reflecting barriers at nodes $j = \pm 15$ on an infinite line. The resulting probability distributions for both CTQW and DTQW are shown in Fig. 5. Both Figs. 5(a) and 5(b) demonstrate similar behavior with the probability distribution mostly confined between the two barriers. Smaller group peaks are observed outside the barriers, which are symmetric about the origin, and their amplitudes depend on the strength of the defect potential Γ_j for CTQW and the phase defect ϕ_j for DTQW. It is interesting to note that the gap between the consecutively transmitted group peaks is simply the distance between the two reflecting barriers, which suggests that the walker is reflected each time it interacts with a defect barrier and consequently bounces back and forth in between. As shown in Fig. 6, the total probability of the quantum walker trapped between the two barriers decreases stepwise as the time increases, with almost constant step time corresponding to the trapping time before significant

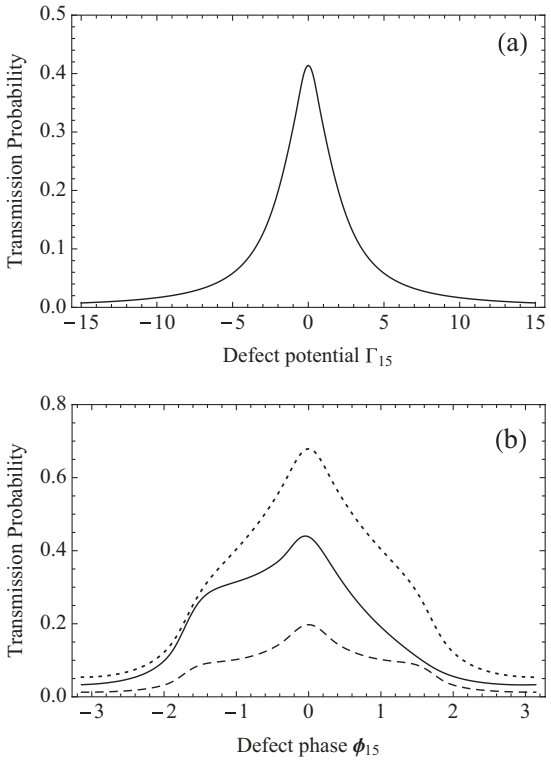

FIG. 4. Transmission probability as a function of (a) the defect potential Γ_{15} for CTQW after time $t = 30$ and (b) the phase defect ϕ for DTQW after $t = 80$ steps. In (b) the solid line corresponds to the coin initial state $(|1\rangle + i|0\rangle)/\sqrt{2}$, whilst the dotted and dashed lines correspond to the coin initial states $|1\rangle$ and $|0\rangle$, respectively.

transmission occurs. The steady emission of group peaks, as shown in Fig. 5, may lead to potential applications such as generating pulses with their magnitudes and time separation controlled by altering the strength and position of the defect barriers.

D. Double defects—resonance

In continuous position space, it has been well established analytically that a quantum particle with energy E incident on double rectangular, cosh, and delta barriers shows complete transmission at particular values of E in the classically forbidden region when $E < V_0$ [31–34]. In this section, we investigate similar resonance behaviors of CTQW in discrete space, in particular on an infinite line with two delta barriers of amplitude α and β placed at vertices $|0\rangle$ and $|L\rangle$. In this case, the Hamiltonian matrix is

$$H = \sum_j (2|j\rangle\langle j| - |j-1\rangle\langle j| - |j+1\rangle\langle j|) + \alpha|0\rangle\langle 0| + \beta|L\rangle\langle L|. \quad (8)$$

Let a momentum eigenstate $|k\rangle$ be incident on the barriers from the left-hand side. The resulting time-independent scattered state $|\psi_s(k)\rangle$ can then be written as [27]

$$|\psi_s(k)\rangle = \begin{cases} |k\rangle + r_1(k)|-k\rangle, & j < 0, \\ t_1(k)|k\rangle + r_2(k)|-k\rangle, & 0 \leqslant j < L, \\ t_2(k)|k\rangle, & L \leqslant j, \end{cases} \quad (9)$$

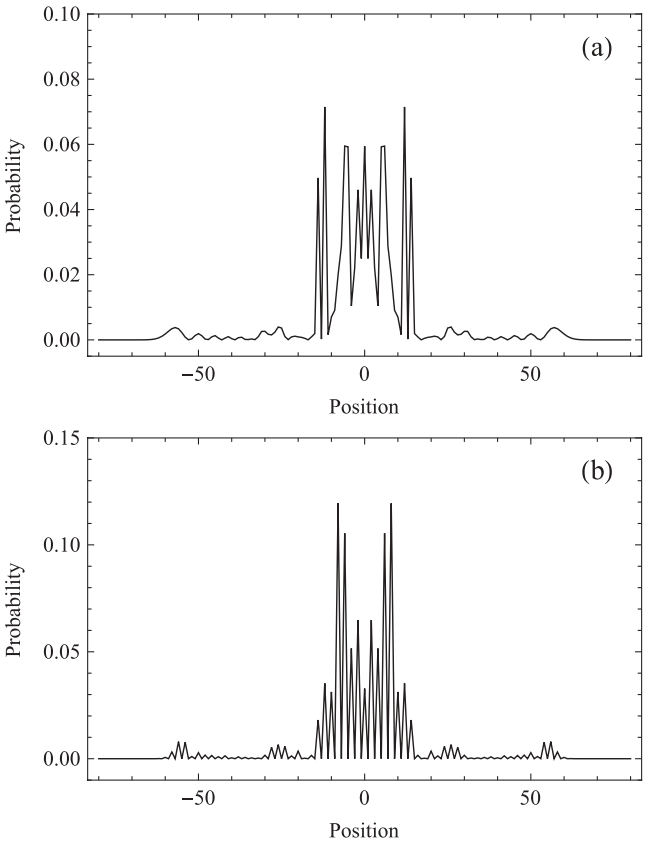

FIG. 5. Probability distribution for a walker initially localized at origin between two barriers for (a) CTQW at time $t = 30$ with the defect potentials $\Gamma_{\pm 15} = 5$, and (b) DTQW after $t = 80$ steps with phase defects $\phi_{\pm 15} = \pi$ and initial state $(|1\rangle + i|0\rangle)/\sqrt{2}$.

where $t_1(k)$ and $t_2(k)$ give the proportion of the momentum eigenstate transmitted through barriers 1 and 2, respectively, and $r_1(k)$, $r_2(k)$ the proportion reflected at each interaction. Recall that, in Sec. II A, it was shown that the orthogonal basis $|k\rangle$ diagonalizes the free Hamiltonian matrix H_0. In the case of double delta barriers, the set of states $|\psi_s(k)\rangle$, $k \in [-\pi, \pi)$ given in Eq. (9) diagonalizes the Hamiltonian $H = H_0 + \Gamma$. Outside the barrier region (i.e., $j \neq -1, 0, L-1, L$), it can be easily shown that

$$\frac{\langle j|H|\psi_s(k)\rangle}{\langle j|\psi_s(k)\rangle} = 2(1 - \cos k).$$

Inside the barrier region (i.e., $j = -1, 0, L-1, L$), the relationship $E(k) = \langle j|H|\psi_s(k)\rangle / \langle j|\psi_s\rangle = 2(1 - \cos k)$ must also hold, which leads to the following system of equations:

$$t_1(k) + r_2(k) - r_1(k) = 1, \quad (10a)$$

$$\frac{e^{2ik}[r_1(k) + t_1(k)] + r_2(k) + 1}{e^{ik}[r_2(k) + t_1(k)]} - \alpha = 2\cos k, \quad (10b)$$

$$\frac{(-1 + 2e^{ik})e^{2ikL}t_1(k) - e^{2ik(L+1)}t_2(k) - e^{3ik}(-2 + e^{ik})r_2(k)}{e^{i(2kL+k)}t_1(k) + e^{3ik}r_2(k)} = 2(1 - \cos k), \quad (10c)$$

$$\frac{r_2(k)e^{-2ik(L-1)} + e^{2ik}t_2(k) + t_1(k)}{e^{ik}t_2(k)} - \beta = 2\cos k. \quad (10d)$$

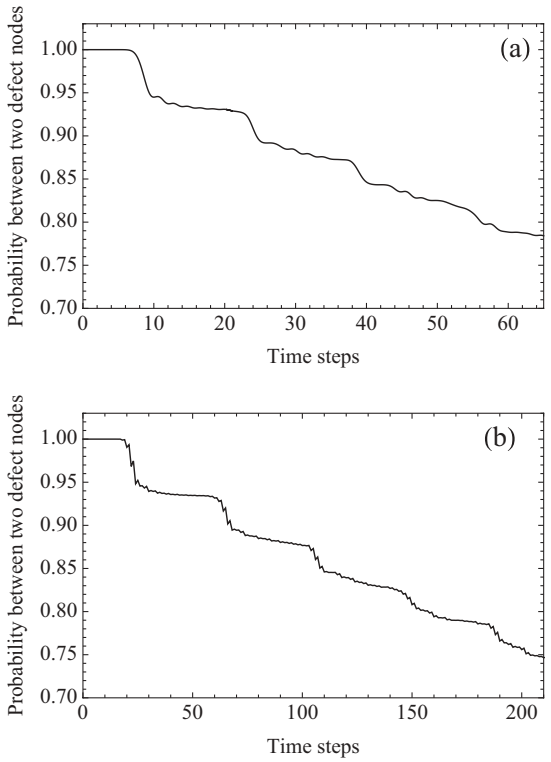

FIG. 6. Trapping probability as a function of time t for (a) CTQW with defect potential $\Gamma_{\pm 15} = 5$, and (b) DTQW with phase defects $\phi_{\pm 15} = \pi$ and initial state $(|1\rangle + i|0\rangle)/\sqrt{2}$.

Equation (10) can be solved to give analytic solutions to $t_1(k)$, $t_2(k)$, $r_1(k)$, and $r_2(k)$—thus producing a set of states $|\psi_s(k)\rangle$ which are eigenstates of H with eigenvalues $E(k) = 2[1 - \cos(k)]$. The transmission coefficient $T(k) = |t_2(k)|^2$ of a momentum eigenstate on an infinite line, incident on two barriers of amplitude α and β, respectively, and separated by distance $L \in \mathbb{N}_0$, is therefore found to be

$$T(k) = \left[1 + \frac{\csc^2 k}{4}(\alpha^2 + \beta^2 + 2\alpha\beta\,\cos 2kL) + \frac{\csc^3 k}{4}\alpha\beta(\alpha+\beta)\sin 2kL + \frac{\csc^4 k}{4}\alpha^2\beta^2\sin^2 kL\right]^{-1}. \tag{11}$$

We also note that a Green's function approach involving transmission and reflection coefficients has been applied to study scattering quantum walks on general graphs, which were shown to be unitarily equivalent to the discrete-time quantum walks [35–38] with the possibility of future work extending this framework to the continuous-time quantum walks. Nevertheless, the above analytical derivation is straightforward and provides the transmission and reflection coefficients in simple forms for quantum walks on the line.

The transmission coefficient is plotted in Fig. 7 over $0 \leqslant k \leqslant \pi$ and for various values of L, α, and β. Oscillating behavior is clearly visible, with the frequency of oscillation increasing rapidly as L increases. It is also observed that when $\beta = 0$ and $L = 0$ (i.e., there is only a *single* barrier of amplitude α) the resonance behavior vanishes—multiple barriers are a necessary condition for CTQW resonance on the infinite line. When $\alpha = 0$ as well, then we are simply observing transmission of a momentum eigenstate in the case of no defects ($H = H_0$) and $T(k) = 1 \forall k$.

By solving the Schrödinger equation with Hamiltonian $H = -\nabla^2 + \alpha\delta(x) + \beta\delta(x + L)$ in continuous space, it can be shown [39,40] that the transmission coefficient is given by

$$T(k) = \left[1 + \frac{\alpha^2\beta^2}{4k^4}\sin kL^2 + \frac{1}{4k^3}2\alpha\beta(\alpha+\beta)\sin 2kL + \frac{1}{4k^2}(\alpha^2 + \beta^2 + 2\alpha\beta\,\cos 2kL)\right]^{-1}. \tag{12}$$

The above equation is identical to Eq. (11) when taking the limit $\csc k \to 1/k$ (the first-order approximation of $\sin k$). The significance of this is twofold. First, with this transformation, the eigenvalue equation $\hat{H}|k\rangle = 2(1 - \cos k)|k\rangle$ becomes $\hat{H}|k\rangle = k^2|k\rangle$, and we recover the energy of a plane wave in continuous space. Second, this relationship highlights the similarity of resonant behavior between quantum dynamical systems and continuous-time quantum walks. The marked differences between the two systems are a result of the finite domain of k, or equivalently the discrete nature of the CTQW position space.

Returning to discrete space, of particular interest is the case $\beta = |\alpha|$, where oscillating resonant behavior is now possible. Solving for $T(k) = 1$ with $\beta = |\alpha|$ in Eq. (11), we find that the distances between defects at which resonance occurs are given by the set

$$L = \begin{cases} n\pi/k + \frac{2}{k}\tan^{-1}\left[\frac{1}{2}\csc(k)(\alpha + \sqrt{\alpha^2 + 4\,\sin^2 k})\right], & \beta = \alpha, \\ n\pi/k, & \beta = -\alpha, \end{cases} \tag{13}$$

where $L, n \in \mathbb{N}_0$. Resonant peaks are illustrated in Fig. 8 as a function of barrier separation L, in the two cases $\alpha = \beta$ and $\alpha = -\beta$.

Special mention should be made of the case $k = \pi/2$, corresponding to a CTQW momentum eigenstate with the largest possible group velocity $[\partial E(k)/\partial k = 2\,\sin k]$. In this instance, the transmission oscillates between two values for successive values of L. Note that when $\alpha = \beta$, there is never perfect transmission; the values oscillate between $T(\pi/2) = 1/(\alpha^2 + 1)$ and $T(\pi/2) = 1/(1 + \alpha^4/4)$ for even and odd L, respectively. However, when $\alpha = -\beta$, perfect transmission occurs for even L, with odd values of L resulting in a reduced transmission of $T(\pi/2) = 1/[1 + \alpha^2(\alpha^2 + 4)/4]$.

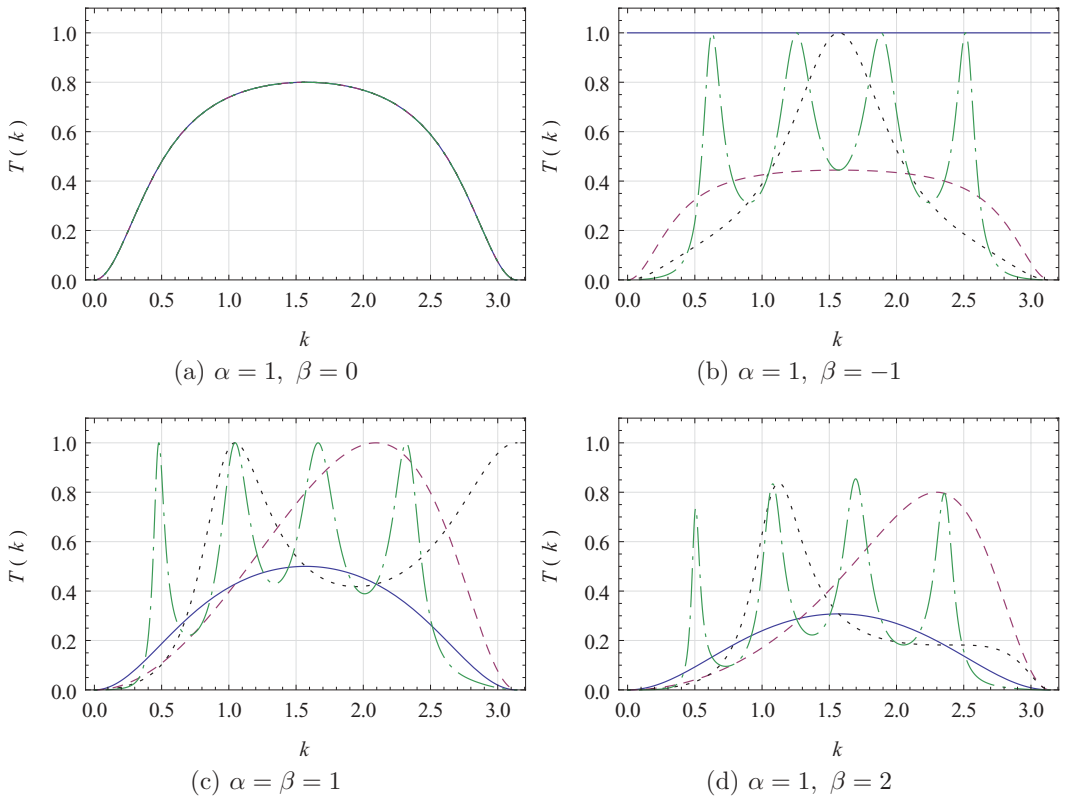

FIG. 7. (Color online) Transmission coefficient vs momentum of a CTQW momentum eigenstate incident on two defects of amplitude α and β, separated by distances $L = 0$ (solid, blue), $L = 1$ (dashed, red), $L = 2$ (dotted, black), and $L = 5$ (dot-dashed, green). The results are shown for the cases (a) $\alpha = 1, \beta = 0$ (i.e., a single defect), (b) $\alpha = 1, \beta = -1$, (c) $\alpha = \beta = 1$, and (d) $\alpha \neq |\beta|$, $\alpha, \beta \neq 0$.

Next consider the boundaries $k \to 0$ and $k \to \pi$. In this case, if $\alpha = -\beta$, transmission occurs only when the two defects overlap and therefore "cancel"each other out, resulting in a free CTQW. When $\alpha = \beta$, we have the following: if $\alpha > 0$, then $\lim_{k\to\pi} T(k) = \delta_{\alpha,2/L}$ and $\lim_{k\to 0} T(k) = 0$; if $\alpha < 0$, then $\lim_{k\to 0} T(k) = \delta_{\alpha,-2/L}$ and $\lim_{k\to\pi} T(k) = 0$.

For other values of k, various forms of "enveloping" in the transmission occur as shown in Fig. 8 for the case $k = 1.45$.

As the CTQW momentum eigenstates $|k\rangle$ form a complete set for the discrete position space, any arbitrary initial state can be decomposed into momenta components—opening the possibility for artificially placed multiple defects

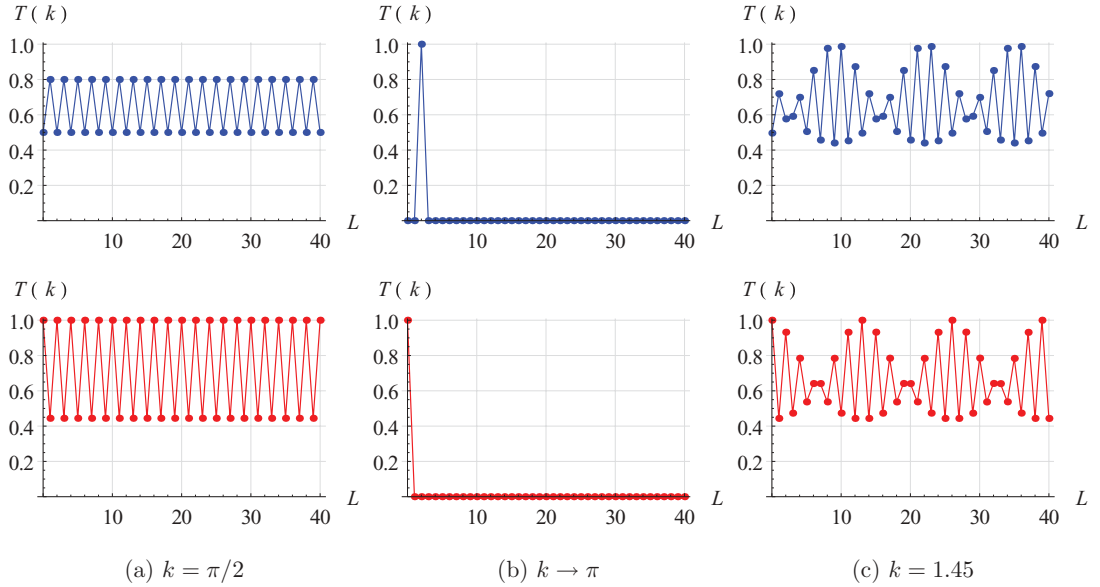

FIG. 8. (Color online) Transmission coefficient $T(k)$ as a function of barrier separation L for momentum eigenstate $|k\rangle$ incident on a double reflecting barrier. Top: $\alpha = \beta = 1$; bottom: $\alpha = -\beta = 1$.

in CTQW systems to selectively control transmission and reflection.

IV. CONCLUSIONS

The quantum walk formalism provides a powerful framework to study the dynamics of quantum particles in a structured discrete position space, while its time evolution can be either discrete (CTQW) or continuous (DTQW). Although the theoretical and physical models of CTQW and DTQW are fundamentally different, their characteristic propagation behavior are often similar. In this paper, detailed comparisons were made between the two models by propagating the quantum walker in both continuous and discrete time on an infinite line in the presence of single or double "defects."

As expected, the delta defect potentials in CTQW cause localization, reflection, transmission, and trapping in a similar way as the quantum wave-packet dynamics in a continuous position space governed by Schrödinger's equation. However, there is no direct analogy of potential barriers in the theoretical formulation of discrete-time quantum walks. In this paper, we demonstrate that adding phase defects in the coin degree of freedom in DTQW plays the same role as the potential barriers in CTQW. We also demonstrate that the effect of altering the phase parameter ϕ in the discrete-time quantum walk is equivalent to changing the barrier strength (Γ) in the continuous-time case. Other definitions of coin phase defects can be equally effective, opening up a wide range of possibilities for the design of efficient quantum-walk-based algorithms.

Moreover, a detailed derivation of the transmission coefficient for the case of a CTQW with a double-point defect is provided, and contrasted to the continuous-space case. It was shown that resonance behavior well established in quantum dynamics extends to the CTQW, with marked differences contributed to the discrete nature of the position space; in particular, under certain conditions only one value of defect separation permits perfect transmission, with perfect reflection occurring for all other integer values of separation.

The effects of disorder and defects on quantum walks are an important field of study, highly relevant in the case of experimental realizations—particularly those with inherent imperfections, or quantum processes which may be unavoidably affected by the environment. As a result of this research, we hope to provide methods to control the spreading of quantum walks, through the use of artificial defects which act to break translational invariance; this could also prove useful in fields such as quantum information processing.

ACKNOWLEDGMENTS

Z.J.L. acknowledges support from the National Nature Science Foundation of China (Grant No. 10974124) and Shanxi Scholarship Council. J.A.I. thanks the John and Patricia Farrant foundation for financial support. We also thank the anonymous referee for providing very constructive comments and suggestions.

[1] J. Kempe, Contemp. Phys. **44**, 307 (2003).
[2] Y. Aharonov, L. Davidovich, and N. Zagury, Phys. Rev. A **48**, 1687 (1993).
[3] E. Farhi and S. Gutmann, Phys. Rev. A **58**, 915 (1998).
[4] R. B. Sessions, M. Oram, M. D. Szczelkun, and S. E. Halford, J. Mol. Biol. **270**, 413 (1997).
[5] M. Mohseni, P. Rebentrost, S. Lloyd, and A. Aspuru-Guzik, J. Chem. Phys. **129**, 174106 (2008).
[6] N. Shenvi, J. Kempe, and K. Birgitta Whaley, Phys. Rev. A **67**, 052307 (2003).
[7] B. L. Douglas and J. B. Wang, J. Phys. A **41**, 075303 (2008).
[8] A. M. Childs, Phys. Rev. Lett. **102**, 180501 (2009).
[9] D. Reitzner, M. Hillery, E. Feldman, and V. Buzek, Phys. Rev. A **79**, 012323 (2009).
[10] S. D. Berry and J. B. Wang, Phys. Rev. A **83**, 042317 (2011).
[11] S. D. Berry and J. B. Wang, Phys. Rev. A **82**, 042333 (2010).
[12] N. V. Prokofev and P. C. E. Stamp, Phys. Rev. A **74**, 020102(R) (2006).
[13] N. Konno, Quantum Inf. Process. **9**, 405 (2010).
[14] P. Törmä, I. Jex, and W. P. Schleich, Phys. Rev. A **65**, 052110 (2002).
[15] Y. Yin, D. E. Katsanos, and S. N. Evangelou, Phys. Rev. A **77**, 022302 (2008).
[16] A. Schreiber, K. N. Cassemiro, V. Potocek, A. Gabris, I. Jex, and C. Silberhorn, Phys. Rev. Lett. **106**, 180403 (2011).
[17] P. W. Anderson, Phys. Rev. **109**, 1492 (1958).
[18] P. Ribeiro, P. Milman, and R. Mosseri, Phys. Rev. Lett. **93**, 190503 (2004).
[19] J. P. Keating, N. Linden, J. C. F. Matthews, and A. Winter, Phys. Rev. A **76**, 012315 (2007).
[20] A. Joye and M. Merkli, J. Stat. Phys. **140**, 1025 (2010).
[21] A. Ahlbrecht, V. B. Scholz, and A. H. Werner, J. Math. Phys. **52**, 102201 (2011).
[22] A. Ahlbrecht, A. Alberti, D. Meschede, V. B. Scholz, A. H. Werner, and R. F. Werner, New J. Phys. **14**, 073050 (2012).
[23] A. Wójcik, T. Łuczak, P. Kurzyński, A. Grudka, T. Gdala, and M. Bednarska-Bzdega, Phys. Rev. A **85**, 012329 (2012).
[24] K. Manouchehri and J. B. Wang, J. Phys. A **40**, 13773 (2007).
[25] O. Mülken, A. Blumen, T. Amthor, C. Giese, M. Reetz-Lamour, and M. Weidemüller, Phys. Rev. Lett. **99**, 090601 (2007).
[26] E. Agliari, A. Blumen, and O. Mülken, Phys. Rev. A **82**, 012305 (2010).
[27] A. M. Childs, E. Farhi, and S. Gutmann, Quantum Inf. Process. **1**, 3543 (2002).
[28] B. Tregenna, W. Flanagan, R. Maile, and V. Kendon, New J. Phys. **5**, 83 (2003).
[29] M. J. Cantero, F. A. Grunbaum, L. Moral, and L. Velazquez, Rev. Math. Phys. **24**, 1250002 (2012).
[30] Reviewer's comment.
[31] P. E. Falloon and J. B. Wang, Comput. Phys. Commun. **134**, 167 (2001).

[32] H. Yamamoto, Y. Kanie, M. Arakawa, and K. Taniguchi, Appl. Phys. A: Solids Surf. **50**, 577 (1990).
[33] K. Manouchehri and J. B. Wang, J. Comput. Theor. Nanos. **3**, 249 (2006).
[34] A. Dutt and S. Kar, Am. J. Phys. **78**, 1352 (2010).
[35] F. M. Andrade and M. G. E. da Luz, Phys. Rev. A **84**, 042343 (2011).
[36] A. G. M. Schmidt, B. K. Cheng, and M. G. E. da Luz, Phys. Rev. A **66**, 062712 (2002).
[37] E. Feldman and M. Hillery, Phys. Lett. A **324**, 277 (2004).
[38] E. Feldman and M. Hillery, J. Phys. A: Math. Theor. **40**, 11343 (2007).
[39] I. Yanetka, Physica B: Condens. Matter **270**, 371 (1999).
[40] I. Yanetka, Acta Phys. Pol. A **116**, 1059 (2009).